

Ordered mesoporous carbons as highly active catalysts for hydrogen production by CH₄ decomposition†

David P. Serrano,^{*ab} Juan Ángel Botas,^{ab} Patricia Pizarro,^a Rut Guil-López^a and Gema Gómez^a

Received (in Cambridge, UK) 10th July 2008, Accepted 17th October 2008

First published as an Advance Article on the web 12th November 2008

DOI: 10.1039/b811800k

Ordered mesoporous carbons have been applied, for the first time, as catalysts for hydrogen production via methane decomposition, showing higher and more stable activity than commercial carbonaceous catalysts.

Since the *hydrogen energy transition* was recognized worldwide as one of the most promising alternatives to carbon-based fuels, great efforts have been dedicated by the scientific community to both production¹ and storage² of hydrogen. A variety of routes to produce hydrogen, such as photocatalytic water splitting,³ are being explored. Thus, catalytic methane decomposition is considered as one of the most promising methods in the short-term since no CO/CO₂ emissions are produced. Moreover, the carbon generated in this process as by-product can be commercialized, thus improving its overall economy¹. Although carbon catalysts operate at higher reaction temperatures than metal-based catalysts, their use may present a number of advantages⁴ such as lower cost of these materials and higher stability against deactivation. A number of carbon materials have previously been checked for methane decomposition, the comparison between their catalytic activities pointing in favour of carbon blacks as these materials combine a high structural disorder and a significant share of accessible surface area^{4–7}.

In the present work, we report for the first time the application of ordered mesoporous carbons as catalysts for methane decomposition exhibiting a high catalytic activity, even superior to that of carbon blacks. In particular, the use of CMK-3 and CMK-5 ordered mesoporous carbons,⁸ characterized by high surface areas and pore structures with hexagonal symmetry (*p6mm*), has been investigated.

CMK-type materials were synthesized according to the literature⁹ by a nano-replication technique, using SBA-15¹⁰ as hard template, furfuryl alcohol (FA) as carbon precursor and oxalic acid (OA) as polymerization catalyst (see ESI† for synthesis and characterization details). In addition to CMK samples, two commercial carbons were used as catalysts: one activated carbon (AC, Merck) and one carbon black (CB-bp, Black Pearls 2000, from Cabot Corp.). They were selected since, according to the

literature, they represent the carbonaceous materials having the highest initial catalytic activity and the strongest resistance to deactivation, respectively, so far tested.^{4–7}

Low-angle XRD patterns of the CMK samples are depicted in Fig. 1. In both cases, (100), (110) and (200) reflections, similar to those of SBA-15 but with lower intensities,¹⁰ can be clearly distinguished, indicating that such carbons have successfully replicated the porous hexagonal symmetry (*p6mm*) of the template. The intensity of the main diffraction peak (100) slightly decreases for the CMK-5 sample, the (110) reflection becoming the most intense one. Although the pore symmetry is analogous for both carbons, they present different structures. CMK-3 consists of arrays of carbon rods, due to the complete filling of the SBA-15 pores with the carbon precursor, whereas CMK-5 is composed of carbon nanotubes formed as a consequence of the partial filling of the template porosity with the carbon precursor.

Fig. 2 shows the N₂ adsorption–desorption isotherms measured at 77 K for the two CMK-type samples. According to the IUPAC classification, they are type-IV isotherms corresponding to the SBA-15 mesostructure replication. Due to the intentional partial infiltration of carbon into SBA-15 pores, an additional adsorption step at higher relative pressures appears for CMK-5, when compared with CMK-3, denoting the existence of a bimodal porosity in the former. This conclusion is confirmed by the pore size distribution determined applying the BJH (Barrett–Joyner–Halenda) model to the adsorption branch of the isotherm (inset in Fig. 2). Thus, while CMK-3 presents a narrow and monomodal mesoporosity centered at about 3 nm, CMK-5 exhibits,

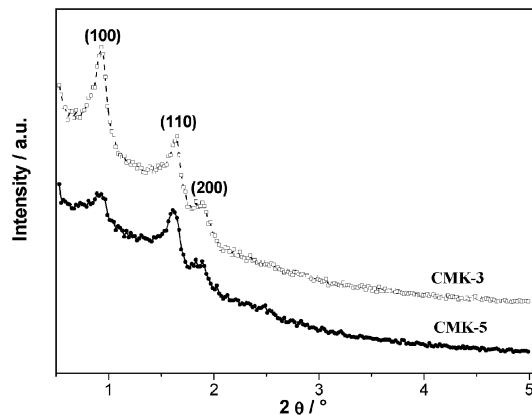


Fig. 1 Low-angle XRD patterns of CMK samples.

^a Department of Chemical and Environmental Technology, ESCET, Universidad Rey Juan Carlos, c/ Tulipán s/n, 28933 Móstoles Madrid, Spain

^b IMDEA Energía, c/ Tulipán s/n, 28933 Móstoles Madrid, Spain. E-mail: david.serrano@urjc.es; Fax: +34 91 488 7068; Tel: +34 91 664 7450

† Electronic supplementary information (ESI) available: Experimental details. See DOI: 10.1039/b811800k

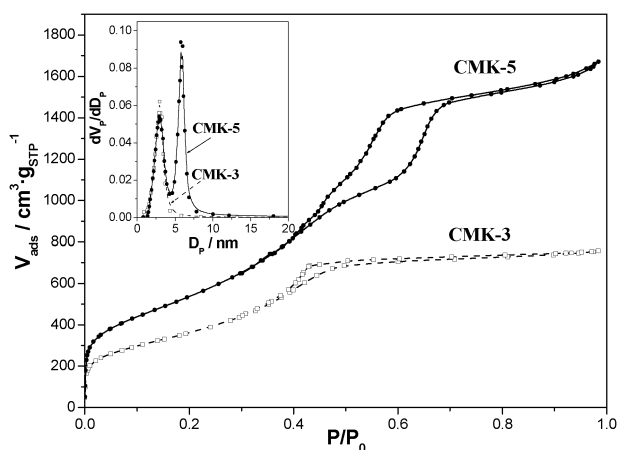


Fig. 2 N₂ adsorption–desorption isotherms and BJH pore size distributions (inset) of CMK samples.

Table 1 Characterization and activity data of carbon catalysts

Carbon	$S_{\text{BET}}/\text{m}^2 \text{g}^{-1}$	$S_{\text{MIC}}/\text{m}^2 \text{g}^{-1}$	$I_{(101)}/I_{(002)}$	$T_{\text{Th}}/^\circ\text{C}$
AC (Activated carbon)	1152	1071	0.84	779
CB-bp (Black Pearls)	1285	988	0.94	778
CMK-3	1323	0	0.53	744
CMK-5	1940	0	0.52	753

in addition to the latter, a second mesoporosity with an average pore size about 5.8 nm.

Table 1 summarizes the textural and structural properties of the different carbon catalysts employed in this work. All samples present BET (Brunauer–Emmett–Teller) surface areas higher than 1000 m² g⁻¹, the largest value (1940 m² g⁻¹) corresponding to CMK-5. Microporosity is negligible for CMK samples, hence their BET areas correspond mainly to the surface area of the mesopores. On the contrary, AC and CB-bp are essentially microporous carbons. Nevertheless, carbon black contains also a significant proportion of external surface (23% for CB-bp *versus* 7% for AC), which is consistent with this material being formed by nanoparticles. On the other hand, from the wide-angle XRD patterns (not shown here) the intensity ratios between the second (101) and first (002) main diffraction peaks of the graphitic framework were calculated. The resultant values, presented also in Table 1, evidence a low degree of graphitization in all carbons, especially for AC and CB-bp samples, which present (101)/(002) ratios close to unity.

The activity of the different carbon catalysts towards methane decomposition was evaluated by thermogravimetric measurements. The sample weight increase due to deposition of the carbonaceous co-product on the catalyst was measured throughout the experiment. Both temperature programmed and isothermal experiments were carried out by passing 100 ml min⁻¹ of the reactive gas (10% CH₄/Ar) through the thermobalance (see ESI† for details).

Fig. 3 illustrates the activity obtained with the carbon catalysts, in terms of hydrogen production relative to the initial mass of catalyst. The activated carbon, although showing a significant initial activity, is quickly deactivated probably

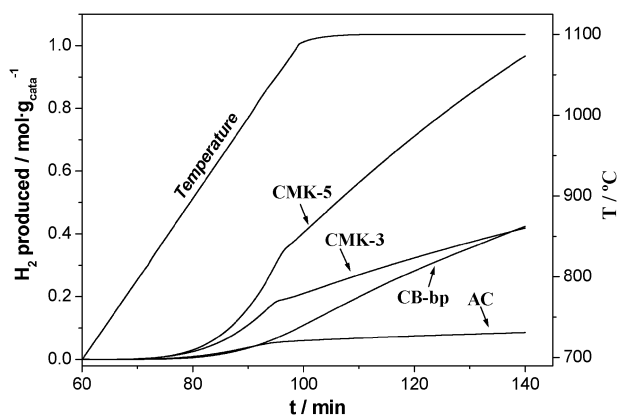


Fig. 3 Evolution of hydrogen production from methane decomposition for different carbon catalysts.

due to a blockage of its microporosity by the carbon deposits. In contrast, the carbon black sample showed a higher resistance to deactivation leading to a stable activity at least during 140 min of reaction. Nevertheless, the highest hydrogen production rates were obtained with the CMK-3 and CMK-5 samples. After about 25 min of reaction, the activity of both carbons underwent a transition, slowing down, but they still kept a significant production of hydrogen. The most remarkable result is the high activity of CMK-5, leading to an overall productivity close to 1 mol of H₂ per gram of catalyst during the progress of the experiment. This production is equivalent to about 22.4 L (STP) of H₂ per gram of catalyst, and it represents twice the value corresponding to CB-bp. Although the catalysts present different pore volume and bed density, the order of catalytic activity is not changed if it is referred to catalyst volume instead of catalyst weight.

For each catalyst, the threshold temperature (T_{Th}) has been estimated as the temperature at which a 0.05% increase of the initial catalyst weight has taken place due to the carbon deposition. This parameter is directly related to the initial activity of the catalysts. Thus, lower T_{Th} values mean higher initial reaction rates. As shown in Table 1, both CMK carbons become active at lower temperatures than the commercial samples. In particular, for CMK-5 the decomposition of methane starts 25 °C below the threshold temperature of CB-bp, in spite of the latter being one of the most active carbon catalysts so far reported in this reaction.

Fig. 4 shows TEM images of the CMK-5 catalyst before and after reaction. In the raw catalyst, the particles possess a high mesoscopic order with a hexagonally arranged pore array. Such particles are metal-free, as corroborated by applying EDX techniques. The image taken after the reaction shows that the carbon deposits, coming from methane decomposition, are located not only inside the pores, but also outside and around the catalyst particles. These deposits are formed by curved and randomly oriented graphene layers having a thickness in the range 3–4 nm. This result suggests that the high and sustained activity of CMK-5 carbon is due to the fact that the carbon deposits formed from the reaction may grow and accumulate on the exterior part of the particles, whereas the active sites located in the mesopores remain accessible to the methane molecules.

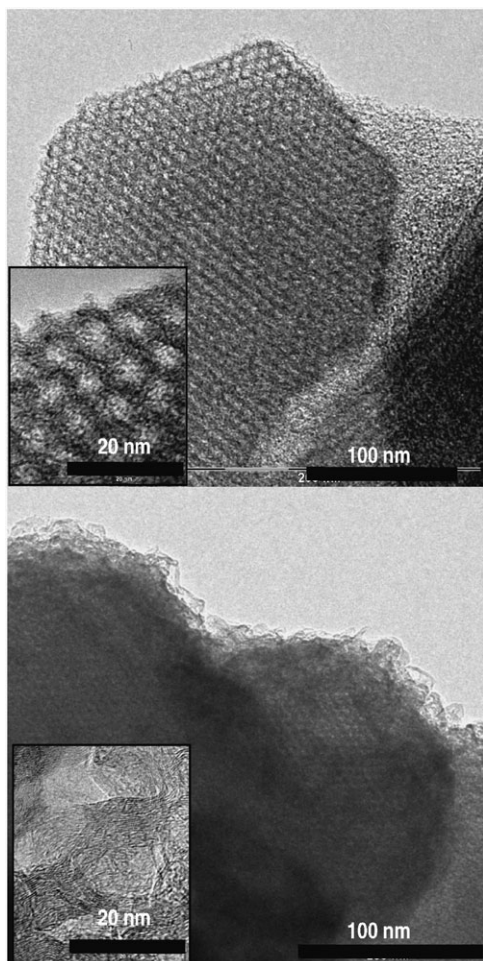


Fig. 4 TEM images of CMK-5 before (top) and after (bottom) the methane decomposition reaction.

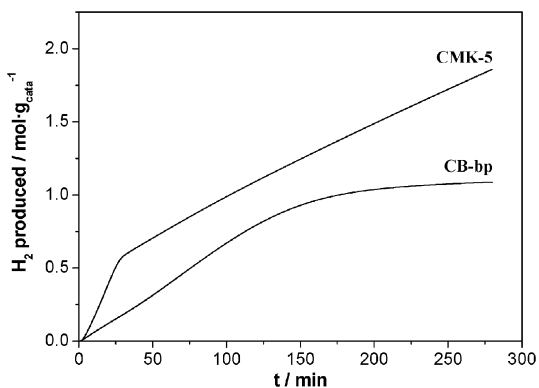


Fig. 5 Evolution of hydrogen production from methane decomposition at 1000 °C using CB-bp and CMK-5 as catalysts.

The long-term stability of CMK-5 and CB-bp catalysts has been checked and compared under isothermal conditions. Fig. 5 represents the resultant hydrogen generation as a function of time for CH₄ decomposition at 1000 °C. While CB-bp was almost completely deactivated after 250 min of reaction, CMK-5 remained highly active after that time. Moreover, when the reaction was extended to 48 h, continuous and significant H₂ generation was still observed for CMK-5.

Interestingly, more than 20 g of carbon deposits per gram of raw catalyst were formed in this experiment. As this amount is clearly superior to that corresponding to the total filling of the CMK-5 porosity, these results confirm that the growth of the carbon formed from the reaction extends towards the outside of the catalyst particles.

The hydrogen production curve for CMK-5 in Fig. 5 shows a two-step linear variation along the reaction time. This indicates that in each step the reaction rate is constant with no autocatalytic behaviour being detected. The transition observed from one step to the other, also present in the temperature programmed experiments, is probably determined by the pore volume available in the CMK-5 catalyst for the growth of the carbon deposits. In the earlier stages of the process, the amount and size of the carbon deposits formed within the catalyst mesopores are rather lower than the volume and diameter of the CMK-5 pores, hence the reaction rate is not influenced by the intraparticle diffusion. However, when the carbon deposits approach in size and volume those of the mesopores, the reaction rate becomes governed by diffusional phenomena. Nevertheless, at this point the porosity of the CMK-5 catalyst is not completely blocked, but is still accessible to the methane molecules as demonstrated by the high long-term activity it exhibits.

In conclusion, here we report the use for the first time of ordered mesoporous carbons as efficient catalysts for the hydrogen production *via* methane decomposition. In particular, the CMK-5 material presents both a high initial activity and a strong resistance to deactivation in spite of the huge amounts of carbon formed as a co-product of the hydrogen production by methane decomposition. The existence of large and uniform mesopores is considered as the main reason for its exceptional activity and stability.

The authors acknowledge “Consejería de Educación, Comunidad de Madrid” as well as “Ministerio de Educación y Ciencia” for supporting this work through the Projects S-0505/EN/0404 (PHISICO2) and ENE2006-06244, respectively. R. Guil also acknowledges the Spanish “Ministerio de Educación y Ciencia” and the European Social Fund for funding her “Ramón y Cajal” contract.

Notes and references

- 1 M. Steinberg, *Energy Convers. Manage.*, 1995, **36**, 791.
- 2 A. W. C. van den Berg and C. Otero Areán, *Chem. Commun.*, 2008, 668.
- 3 F. A. Frame, E. C. Carroll, D. S. Larsen, M. Sarahan, N. D. Browning and F. E. Osterloh, *Chem. Commun.*, 2008, 2206.
- 4 N. Muradov, F. Smith and A. T-Raissi, *Catal. Today*, 2005, **102–103**, 225.
- 5 N. Muradov, *Catal. Commun.*, 2001, **2**, 89.
- 6 I. Suelves, M. J. Lázaro, R. Moliner, J. L. Pinilla and H. Cubero, *Int. J. Hydrogen Energy*, 2007, **32**, 3320.
- 7 J. Ashok, S. Naveen Kumar, A. Venugopal, V. Durga Kumari, S. Tripathi and M. Subrahmanyam, *Catal. Commun.*, 2008, **9**, 164.
- 8 R. Ryoo, S. H. Joo; S. Jun, T. Tsubakiyama and O. Terasaki, *Stud. Surf. Sci. Catal.*, 2001, **135**, 1121.
- 9 P. A. Bazula, A.-H. Lu, J.-J. Nitz and F. Schüth, *Microporous Mesoporous Mater.*, 2008, **108**, 266.
- 10 D. Zhao, J. Feng, Q. Huo, N. Melosh, G. H. Fredrickson, B. F. Chmelka and G. D. Stucky, *Science*, 1998, **279**, 548.